Structural origins of constitutive activation in rhodopsin: Role of the K296/E113 salt bridge

Jong-Myoung Kim[†], Christian Altenbach[‡], Masahiro Kono[§¶], Daniel D. Oprian[§‖], Wayne L. Hubbell[‡‖], and H. Gobind Khorana[†‖]

[†]Departments of Biology and Chemistry, Massachusetts Institute of Technology, Cambridge, MA 02139; [‡]Jules Stein Eye Institute and Department of Chemistry and Biochemistry, University of California, Los Angeles, CA 90095; and [§]Department of Biochemistry, Brandeis University, Waltham, MA 02454

Contributed by H. Gobind Khorana, June 29, 2004

The intramolecular interactions that stabilize the inactive conformation of rhodopsin are of primary importance in elucidating the mechanism of activation of this and other G protein-coupled receptors. In the present study, site-directed spin labeling is used to explore the role of a buried salt bridge between the protonated Schiff base at K296 in TM7 and its counterion at E113 in TM3. Spin-label sensors are placed at positions in the cytoplasmic surface of rhodopsin to monitor changes in the structure of the helix bundle caused by point mutations that disrupt the salt bridge. The single point mutations E113Q, G90D, and A292E, which were previously reported to cause constitutive activation of the apoprotein opsin, are found to cause profound movements of both TM3 and TM6 in the dark state, the latter of which is similar to that caused by light activation. The mutant M257Y, which constitutively activates opsin but does not disrupt the salt bridge, is shown to cause related but distinguishable structural changes. The double mutants E113Q/M257Y and G90D/M257Y produce strong activation of the receptor in the dark state. In the E113Q/M257Y mutant investigated with spin labeling, the movement of TM6 and other changes are exaggerated relative to either E113Q or M257Y alone. Collectively, the results provide structural evidence that the salt bridge is a key constraint maintaining the resting state of the receptor, and that the disruption of the salt bridge is the cause, rather than a consequence, of the TM6 motion that occurs upon activation.

G protein-coupled receptor | signal transduction | EPR | site-directed spin labeling

Rhodopsin, the vertebrate dim-light photoreceptor, is the prototypic and best-studied member of the largest known superfamily of cell surface receptors, the G protein-coupled receptors. These receptors all contain seven transmembrane helical segments (TM1–TM7), as was clearly established in early structural studies of rhodopsin by cryoelectron microscopy (1) and confirmed more recently at higher resolution in 3D x-ray crystal structures of the dark state of the protein (2–4). In addition to the seven transmembrane helices, the x-ray structures reveal a short eighth helix in the C-terminal segment of the protein lying along the cytoplasmic surface of the membrane (H8, Fig. 1 *A* and *B*).

The chromophore in rhodopsin, 11-*cis*-retinal, is bound to the protein covalently by means of a protonated Schiff linkage to the ε-amino group of Lys-296 located in TM7. The buried positive charge on the Schiff base nitrogen is stabilized by an electrostatic interaction, a salt bridge, with the charged carboxylate of Glu-113 in TM3 (Fig. 1*C*) (5–7). Capture of a photon by rhodopsin results in isomerization of retinal to the *all-trans* form. The isomerization triggers a series of transient conformational changes in the protein culminating in the formation of metarhodopsin II (MII), the active conformation (8). Concomitant with the formation of MII, the Schiff base nitrogen is deprotonated (9) and the Glu-113/Lys-296 salt bridge is broken.

The role of the salt bridge in determining the structure of rhodopsin and whether the rupture of the salt bridge is a cause or consequence of the protein conformational change leading to MII are unknown. However, the existence of mutations that apparently disrupt the Glu-113/Lys-296 salt bridge and constitutively activate the apoprotein, opsin, suggest that the former possibility may be the case (10–12). Two such mutations are in Glu-113 and Lys-296 themselves that directly disrupt the Glu-113/Lys-296 salt bridge. Two other mutations are in amino acids Gly-90 and Ala-292 located in TM2 and TM7, respectively. When mutated to Asp-90 or Glu-292, the newly introduced carboxylate side chain is spatially positioned in the structure to compete with Glu-113 for the positive charge on Lys-296 (Fig. 1*C*), thus potentially rupturing the salt bridge by a competitive mechanism (13, 14). This group of mutations is of interest not only with regard to the mechanism of activation of the protein, but also because three of the four mutations have been identified as the causative lesions of two different inherited diseases of the retina: retinitis pigmentosa (K296E, M) (15, 16) and congenital stationary night blindness (G90D and A292E) (13, 17). None of these mutations cause activation of the dark state of the protein with bound 11-*cis*-retinal.

Other mutations that cause constitutive activation of opsin but that do not in any obvious way effect the K296/E113 salt bridge are known (18–20). Among these mutants are M257Y on the inner surface of TM6 (18) and E134Q at the cytoplasmic termination of TM3 (19, 20) in the highly conserved D(E)RY sequence in rhodopsin family G protein-coupled receptors (Fig. 1 *A* and *B*). As for the salt-bridge mutants mentioned above, these mutations do not lead to activation of the receptor containing 11-*cis*-retinal but only of the unliganded receptor. On the other hand, the double mutations E113Q/M257Y, E113Q/M257N, and E113Q/M257A produce strong activation of rhodopsin in the dark state (18).

To determine structural changes in rhodopsin induced by the mutations M257Y, E113Q, A292E, G90D, E134Q/M257Y, and E113Q/M257Y, site-directed spin labeling (21–25) is used. To monitor the status of the rhodopsin helix bundle, a sensor nitroxide side chain, designated as R1 (Fig. 2), was introduced at sites 140, 227, 250, or 316 at the cytoplasmic ends of TM3, TM5, TM6, and H8, respectively (Fig. 1 *A* and *B*). Earlier studies have shown that EPR spectral changes for R1 at these sites, which arise from changes in nitroxide mobility, provide a diagnostic signature for formation of the activated state of rhodopsin (26, 27). Major structural changes reported by 227R1 and 250R1 have been interpreted to result from a rigid-body displacement of TM6 toward TM5, as indicated by the arrow in Fig. 1*B*. This result is strongly supported by other side-chain mobility changes throughout the TM5–TM6 cytoplasmic region (28) and by direct measurement of changes in interhelical distances upon photoactivation (29). Importantly, crosslinking

[¶]Present address: Department of Ophthalmology, Medical University of South Carolina, Charleston, SC 29425.

[‖]To whom correspondence may be addressed. E-mail: khorana@mit.edu, oprian@brandeis.edu, or hubbellw@jsei.ucla.edu.

www.pnas.org/cgi/doi/10.1073/pnas.0404519101

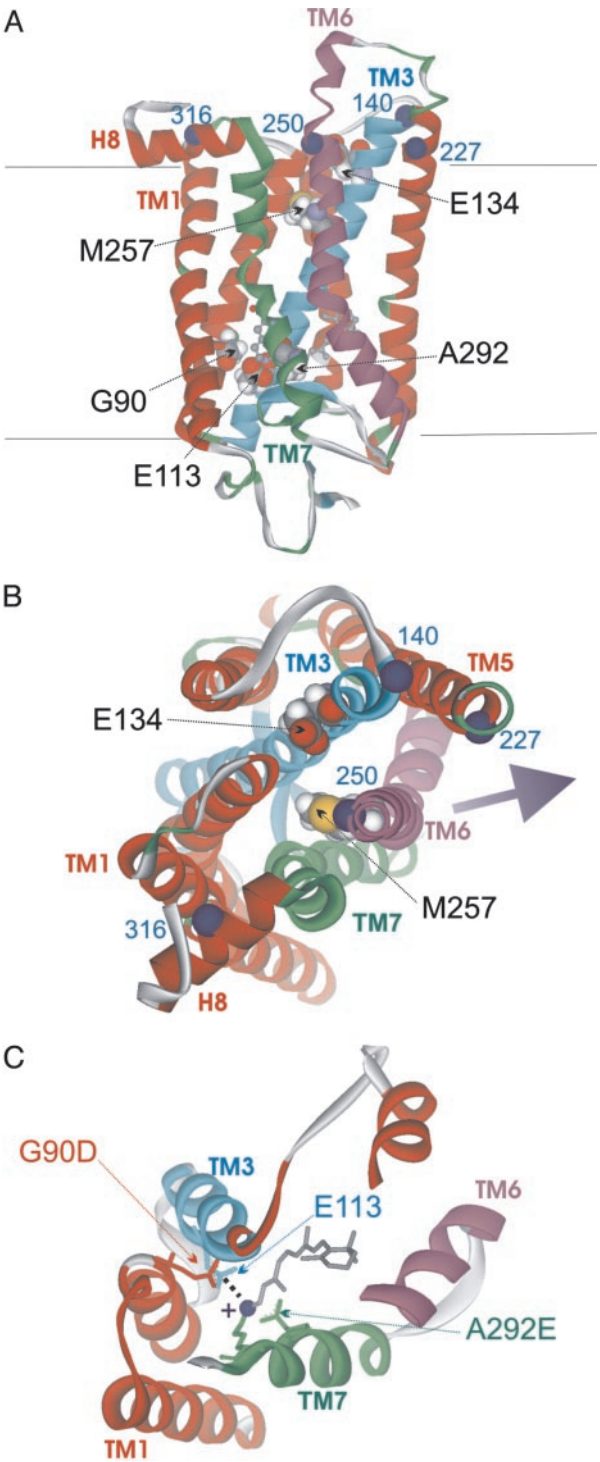

Fig. 1. The structure of rhodopsin and locations of constitutively active and sensor mutations. (*A*) Side view of the rhodopsin structure indicating transmembrane helices 1, 3, 6, and 7, and helix 8 lying parallel to the cytoplasmic surface of the membrane. The residues mutated (90, 113, 134, 257, and 292) are shown as space-filling models, and the positions of the R1 sensors are indicated by blue sphere at the alpha carbon atom. The horizontal lines indicated the location of the membrane–solution interfaces. (*B*) Cytoplasmic view of the rhodopsin structure. The arrow indicates the direction of motion of TM6 upon photoactivation. (*C*) Extracellular cutaway view of the rhodopsin structure, showing the locations of Glu-113 and the G90D and A292E mutations. The native Glu-113/Lys-296 salt bridge is shown as a dashed line. The mutated side chains and the retinal chromophore (gray) are modeled as stick figures. The blue sphere indicates the amino group of Lys-296. (All models are based on PDB entry 1GZM.)

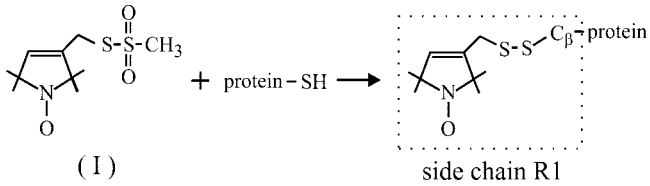

Fig. 2. The reaction of methanethiosulfonate reagent to generate the nitroxide side chain R1.

experiments show that displacement of TM6 is an essential component of receptor activation (29, 30). Smaller but significant changes also are detected by 140R1 at the TM3–TM5 interface and 316R1 at the TM1–H8 interface (31, 32).

As reported below, the mutations E113Q, G90D, and A292E in the dark state of rhodopsin each produce a pattern of structural changes, sensed by the spin labels, that is strikingly similar to that produced by light activation of the wild-type receptor but with an amplified change detected at the TM3–TM5 interface. M257Y produces a distinctive pattern of changes indicating a fundamentally different structural origin. The double mutant E113Q/M257Y, which constitutively activates the dark state, produces amplified changes at all sites, compared with the individual mutations.

Materials and Methods

Cloning, Expression, Purification, and Spin Labeling of Rhodopsin Mutants. Plasmids encoding the point mutations G90D, E113Q, A292E, and M257Y were prepared as described in refs. 5 and 10–14. Plasmids encoding cysteine replacements C316S, V227C/C140S/C316S, V250C/C140S/C316S, or C140S were prepared as described in refs. 32 and 33; proteins expressed from these plasmids contain a single cysteine reactive to reagent (I) at sites 140, 227, 250, or 316, respectively. All plasmids are derivatives of pMT3 or pMT4.

Plasmids encoding G90D together with a reactive cysteine at sites 140, 227, 250, or 316 were obtained by combinations of a 5.6-kb *Xho*I–*Not*I fragment of the G90D plasmid with 0.7-kb *Xho*I–*Not*I fragments of plasmids containing one of the above cysteine replacements. Plasmids encoding E113Q with a cysteine at one of the above sites were obtained by ligation of a 0.9-kb *Bsa*AI fragment of the E113Q plasmid with a 5.4-kb *Bsa*AI fragment of the plasmid containing the desired cysteine replacement. Plasmids containing the M257Y or A292E mutation together with a single cysteine replacement were obtained by ligation of a 0.2-kb *Mlu*I–*Bsp*EI fragment of the A292E or M257Y plasmid with a 6.1-kb *Mlu*I–*Bsp*EI fragment from the plasmids containing the cysteine replacement.

Plasmids containing double mutations were constructed by combinations of restriction fragments containing each mutation. The fragments combined were as follows: 715- and 5,467-bp *Xho*I/*Not*I (G90D/M257Y), 298- and 5,884-bp *Mlu*I/*Not*I (E113Q/M257Y and E134Q/M257Y), and 388-bp *Eco*RI/*Bsa*I together with 471-bp *Apa*I/*Bsa*I and 5,323-bp *Apa*I/*Eco*RI (E113Q/E134Q). Plasmids containing the double mutants together with a single cysteine in the cytoplasmic domain of rhodopsin were constructed by replacements of restriction fragments (34) containing the desired mutations.

Procedures for protein expression in COS-1 cells, purification on columns of 1D4 Sepharose, spin labeling with reagent, and recording of EPR spectra are described in refs. 32 and 34.

Assay for Transducin Activation. Transducin was extracted from rod outer segment preparations and purified by DE52 column chromatography as described in ref. 35. Transducin activation was assayed in a mixture containing 10 mM Tris·Cl (pH 7.4), 100

BIOPHYSICS

Table 1. Comparison of initial rates for transducin (Gt) activation by rhodopsin mutants

Mutant*	Gt Activation,† % Dark	Gt Activation,† % Light	Refs.
Wild type	1	100	
E134Q	1.5 ± 0.2	103 ± 5	20
M257Y	2 ± 0.2	106 ± 0.5	18
E113Q	2.5 ± 0.5	96 ± 5	5, 6
A292E	0.6 ± 0.2	88 ± 5	13
G90D	0.9 ± 0.2	65 ± 5	14
E134Q/M257Y	3 ± 0.5	105 ± 5	—
E113Q/E134Q	6 ± 2	105 ± 10	18
E113Q/M257Y	70 ± 5	105 ± 10	18
G90D/M257Y	40 ± 5	105 ± 10	—

*The mutants were regenerated with 11-*cis*-retinal, purified in 2 mM NaPi (pH 6.0)/0.05% DM, and then assayed for Gt activation as described in *Materials and Methods.*

†Values given as percent of wild-type activation.

mM NaCl, 0.5 mM $MgCl_2$, 0.015% dodecyl maltoside, 2 nM rhodopsin, 0.5 μM transducin, and 3 μM GTP-γ^{35-}S (specific activity ≈5,000 cpm/pmol), as described in ref. 36. Aliquots taken at various time points were added to 150 μl of 10 mM Tris·Cl (pH 7.5), 100 mM NaCl, 10 mM EDTA, and 10 μM GTPγS to stop the reaction. After transferring the solution to a nitrocellulose membrane, each blot was washed twice with a buffer containing 10 mM Tris·Cl (pH 7.5) and 100 mM NaCl. The nitrocellulose filters were dried, and the radioactivity was measured by Cerenkov counting after the addition of 5 ml of scintillation fluid. Transducin activation was expressed as the cpm relative to that obtained with wild-type rhodopsin.

Results

Characterization of the Mutants. The mutants E113Q, G90D, A292E, E134Q, M257Y, E113Q/E134Q, and E113Q/257Y were previously reported and characterized with respect to constitutive activation (Table 1). The new double mutants E134Q/M257Y and G90D/M257Y formed chromophores in the dark upon addition of 11-*cis*-retinal that had UV/Vis spectra similar to that of wild-type rhodopsin. In each case, photolysis produced a mixture of pigments with absorption maxima near 380 and 480 nm (Fig. 3 *A* and *B*).

Table 1 presents data obtained in the present study for transducin activation for the dark and light-activated states of all mutants investigated, together with references to previous studies on the relevant mutants. In agreement with published data, E134Q, M257Y, E113Q, A292E, and G90D in the dark state showed little activation of transducin and relatively normal activation in the light. Similarly, the double mutants E134Q/M257Y and E113Q/E134Q showed little activation of transducin in the dark. On the other hand, E113Q/M257Y and G90D/M257Y in the dark state show 70% and 40%, respectively, of the transducin activation produced by native light-activated rhodopsin.

Conformational Changes in Rhodopsin Due to the Salt-Bridge Mutants E113Q, G90D, and A292E. To monitor structural changes in rhodopsin due to the mutations listed in Table 1, each single mutation and the double mutations E113Q/M257Y and E134Q/M257Y were introduced into rhodopsin along with a single R1 side chain at sites 140, 227, 250, or 316 (Fig. 1 *A* and *B*). Rhodopsin containing a single spin label at sites 140, 227, 250, or 316 with no additional mutations will be referred to as WT*. E113Q/M257Y and E134Q/M257Y were selected for structural analysis to represent double mutations that cause and do not cause, respectively, constitutive activation of the dark state of the receptor.

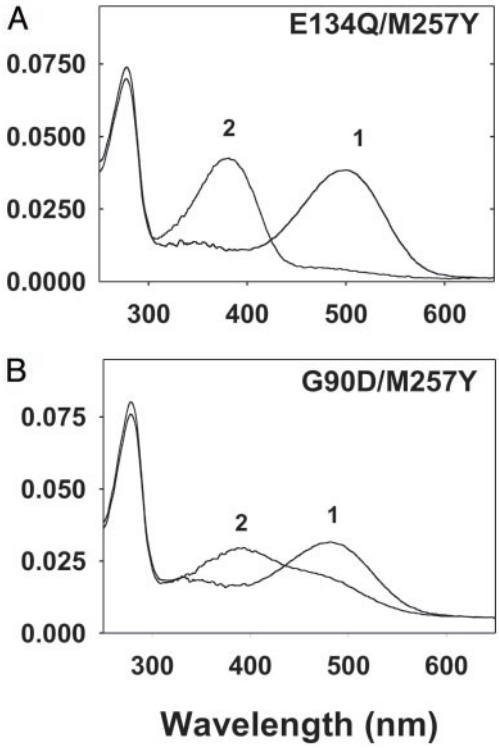

Fig. 3. UV/Vis spectra of the indicated double mutants recorded in the dark (trace 1) and within 1 min after illumination for 30 sec with light filtered by a long-pass filter ($\lambda > 495$ nm) (trace 2). The mutants were purified in 2 mM NaPi (pH 6.0)/0.05% DM after regeneration with 10 mM 11-*cis*-retinal.

Fig. 4 shows the low field half of the EPR spectra for each R1 sensor in the mutants investigated. For reference, Fig. 4*A* shows

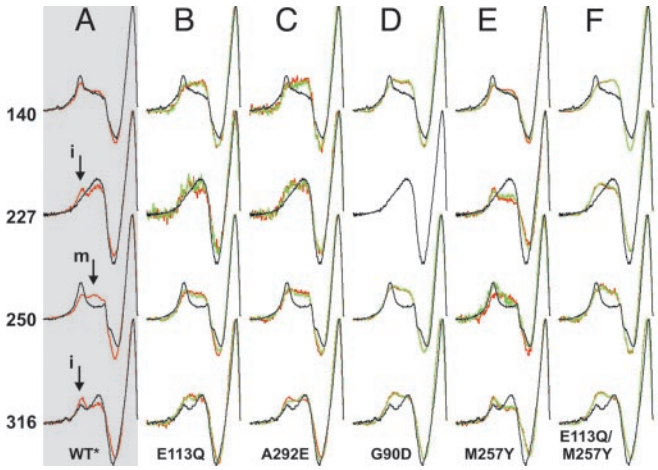

Fig. 4. EPR spectra of the indicated sensor mutant in the dark and after photoactivation for the wild-type (*A*) and constitutively active mutants (*B–F*). For clarity, only the low-field half of each spectrum is shown. The arrows identify regions corresponding to mobile (m) and immobile (i) nitroxides. All spectra are normalized to the height of the center resonance line to compare the lineshapes. Photoactivation for WT*, A292E, G90D, and M257Y was accomplished by illumination for 30 sec with light from an infrared-filtered 75-W halogen source additionally filtered with a long-pass filter transmitting at >500 nm. For E113Q and E113Q/M257Y, photoactivation was carried out with light from the same source but additionally filtered with a band-pass filter centered at 400 nm (±50 nm).

the EPR spectra for the WT* receptors, both in the dark and the light. These spectra are essentially identical to those previously reported, and the dark–light differences reflect the activating conformational change triggered by light. Detailed analyses of the spectral changes have been discussed elsewhere. Briefly, the R1 sensor at position 140 reports a small but reproducible shift of the nitroxide population to a more mobile state in the activated state of the receptor (32), reflecting changes near the TM3–TM5 interface where 140R1 resides (Fig. 1*B*). The spectral changes at sites 227 and 250 together identify the major feature of the conformational switch, the outward movement of TM6 by ≈8 Å (28, 29). The TM6 movement engages 227R1 in tertiary interaction and at the same time removes such interactions at 250R1, accounting for the decrease and increase, respectively, in mobility of R1 at the two sites. The changes in mobility at 227R1 and 250R1 are revealed in the EPR spectra by increases in the intensities of components corresponding to immobilized (i) and mobile (m) populations, respectively (Fig. 4*A*, arrows). Finally, for 316R1 in H8, the population shifts to a more immobilized state upon activation (Fig. 4*A*, arrows), indicating reorganization at the H8–TM1 interface (32). Measurements of changes in interhelical distances suggest that movement in this region is small in comparison with that of TM6 (37).

Fig. 4 *B–D* shows the low field half of the EPR spectra for R1 at each sensor position in the three salt-bridge mutants, G90D, E113Q, and A292E, in the dark (green) and light-activated states (red), together with those for the dark state of the corresponding WT* receptor for comparison (black). As is evident, the mutations result in a striking pattern of changes in the structure of the dark state that is essentially identical in each and is very similar to that produced by photoactivation in the WT* receptor as reported by sensors 227R1, 250R1, and 316R1. The spectra for 227R1 in the salt-bridge mutants are relatively noisy, and in the case of G90D, the signal was too low to record a reliable EPR spectrum (Fig. 4*D*). Because the amount of protein in the sample was similar for each (≈0.4 nmol), the yield of the labeling reaction for 227C apparently was low.

Interestingly, the sensor 140R1 shows a change due to the salt-bridge mutations that is similar in type (i.e., an increase in a mobile population of R1) but of much larger magnitude than that observed upon photoactivation of the WT* protein. Finally, it is significant that the sensors detect relatively small changes in the salt-bridge mutants upon exposure to light and isomerization of retinal, indicating that much of the structural change (as monitored at these positions) has already been produced in the dark by the mutation. Although small, a residual change upon photoactivation can be seen for 250R1, 316R1, E113Q, and A292E, but not for G90D. Even though the additional change due to light activation is small, it is apparently significant in a functional sense, because these mutations do not activate the dark state of rhodopsin in DM (5, 6, 10, 11, 13, 14) (Table 1).

Conformational Changes in Rhodopsin Due to M257Y and E134Q/M257Y. Other constitutively activating mutations, which do not directly perturb the salt bridge in rhodopsin, include E134Q and M257Y. Previous studies of E134Q with R1 at sites 140, 227, 250, or 316 revealed a fundamentally different pattern of changes in the dark state, compared with those for the salt-bridge mutants discussed (26). Specifically, changes were reported only by 140R1 and 316R1. The EPR spectra for the nitroxide sensors in the M257Y mutant shown in Fig. 4*E* also are different from those seen with the salt-bridge mutants. In M257Y, essentially full changes characteristic of light activation are sensed by 227R1 and 316R1 in the dark state, with an additional small change at 227R1 upon exposure to light, but no further change at 316R1. The 140R1 sensor reports small changes in the dark state structure due to the mutation but retains a small, light-dependent change characteristic of the wild-type protein. Relatively small changes are sensed by 250R1 in the dark state that are in the direction of those produced by light activation of the wild type, and an additional change is seen upon light activation of the mutant. Thus, this mutation produces a pattern of helix movements that are fundamentally different from that due to the salt-bridge mutants and light activation of the WT* receptor.

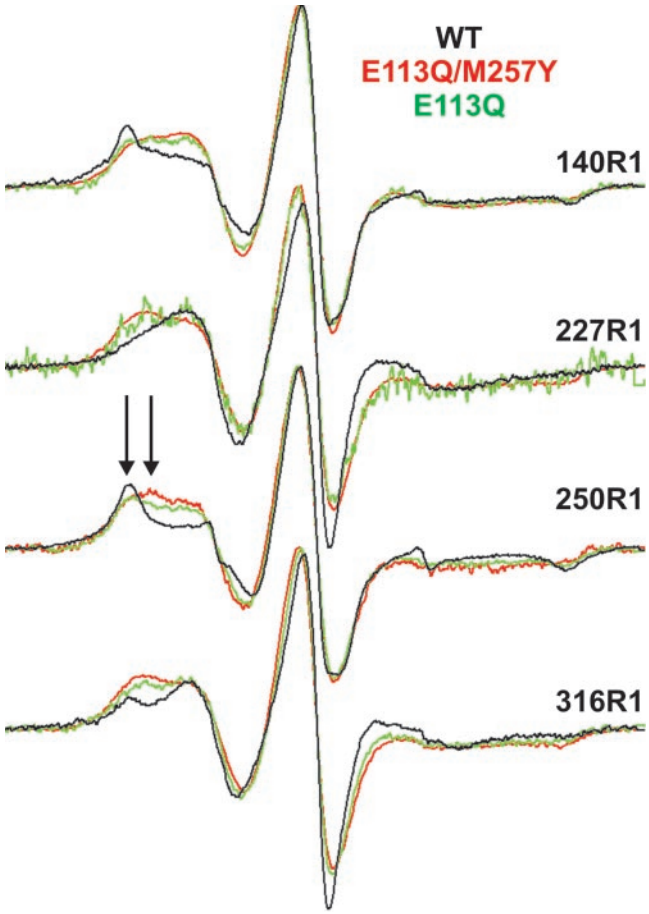

Fig. 5. Comparison of the EPR spectra for the R1 side chain at sites 140, 227, 250, and 316 for WT* rhodopsin (black trace), the double-mutant E113Q/M257Y (red trace), and E113Q (green trace). The full EPR spectra, normalized to the height of the center line (peak-to-peak), are shown.

The double mutant E134Q/M257Y, a combination of mutants that do not directly affect the salt bridge, has EPR spectra for the nitroxide sensors essentially identical to those of the M257Y single mutant (data not shown). This result is not surprising for sensors 227R1 and 250R1, because the E134Q mutant produces no effect at these sites (26). On the other hand, E134Q produces effects at 140R1 and 316R1 that are equivalent to those of M257Y alone. Thus, the structural effects of these mutants are apparently not additive, at least at sites 140 and 316.

Conformational Changes in Rhodopsin Due to E113Q/M257Y. Double mutants E113Q/M257Y and G90D/M257Y contain combinations of mutants that disrupt the salt bridge (E113Q and G90D) and one mutant that does not (M257Y). These unique mutants result in constitutive activity in the dark state (Table 1). E113Q/M257Y, which was selected for investigation by using the nitroxide sensor mutants, produces changes in the dark state that resemble in type those produced by E113Q alone (Fig. 4*F*). However, the changes are exaggerated in comparison with those of either individual mutant alone. The difference is shown in Fig. 5, which compares the full spectra for the dark states of the WT*

(blue trace), E113Q (green trace), and E113Q/M257Y (red trace). Although the difference is small at site 140, the differences are apparent at the important sites 227 and 250, which detect TM6 motion, and large at site 316 in H8. When compared with M257Y alone, the differences are even larger (data not shown). The effects of the two mutations appear to be approximately additive. Importantly, additional effects due to light activation are abolished at all sites (Fig. 4*F*), and the yield of the spin-labeling reaction at site 227 is high in this mutant.

Discussion

The E113Q, A292E, and G90D Mutants and the Role of the K296/E113 Salt Bridge in Receptor Activation. The Lys-296/Glu-113 salt bridge in rhodopsin is broken in the E113Q mutant, and the results presented in this study directly demonstrate the structural consequences of this event. As shown in Fig. 4, the rupture of the salt bridge in the E113Q mutant results in a movement of TM6 and other changes in the dark receptor that are very similar to those induced by photoactivation of the WT* protein. These data show that the salt bridge is a primary constraint that determines the position of the cytoplasmic region of TM6. Because motion of TM6 is believed to be necessary for receptor activation (29, 30), it appears that a direct and primary result of photoisomerization of retinal is to break this salt bridge, and this may be the fundamental trigger for activation. A simple mechanistic link between rhodopsin and other G protein-coupled receptors may be imagined whereby binding of the agonist ligand, rather than photoisomerization of a tightly bound chromophore, makes or breaks a critical salt bridge or some other energetically equivalent interaction.

It is most remarkable that the structural changes produced by mutants E113Q, G90D, and A292E are so similar to each other. The changes observed by the various sensors for the E113Q mutant, in which the Schiff base of the chromophore is deprotonated (5–7) and the salt bridge between Glu-113 and the Lys-296 is directly broken, are almost exactly duplicated by mutations in which a potential negative charge is placed at site 90 or 292. This strongly supports the proposal that the mutations at sites 90 and 292 also break the salt bridge but by an indirect competitive mechanism in which the introduced carboxylate competes with Glu-113 for the charge on the Schiff base nitrogen (Fig. 1*C*). Whereas visible absorption spectroscopy indicates that the Schiff base nitrogen is protonated in the G90D and A292E mutants (13, 14), it is thus likely that the positive charge is stabilized by interaction with the carboxylate at sites 90 or 292 but not at 113, a conclusion that is also in agreement with Fourier transform infrared spectroscopy studies (38).

An important difference between the effects of light activation and the salt-bridge mutants in the dark is seen by the sensor 140R1, which registers a much larger structural change at the TM3–TM5 interface in the mutants than that due to light activation in the WT*. One interesting model to account for this result is that a weak interaction persists between E113 and K296 (or other group) in the WT* receptors in the activated state that is abolished in the mutants. For example, a weak hydrogen bond or solvent-separated H bond may exist between E113 and K296 after proton transfer from the latter to the former upon MII formation.

Another important difference between the light-activated WT* receptor and the salt-bridge mutants in the dark state is that the salt-bridge mutants are not activated with respect to transducin activation. This finding implies that there are additional constraints on the receptor structure that must be modified to reach the active conformation. Indeed, small but reproducible structural changes due to light activation are seen in the mutants E113Q and A292E that presumably reflect the removal of constraints due to changes in the chromophore geometry upon isomerization. Similar light-induced structural changes are not seen in G90D, perhaps related to the relatively small effect of light activation in this receptor mutant (Table 1).

Each of the single salt-bridge mutants has a relatively low yield of the labeling reaction at 227C. As noted above, 227R1 experiences an increased tertiary interaction with TM5 in the activated state, and a cysteine at this site would be expected to have reduced accessibility to the nitroxide reagent. Thus, the low reactivity is consistent with the idea that the salt-bridge mutants induce a conformation that mimics the activated state.

Other Mutants That Constitutively Activate Opsin. If rupture of the salt bridge is the fundamental cause of the structural changes registered by the R1 sensors in the WT* protein, then constitutively activating mutations that do not directly affect the salt bridge should function by an alternative mechanism and should result in EPR changes that are qualitatively different from those observed with the salt-bridge mutants. In accord with this expectation, the previously published results for the E134Q mutant (26) and those for the M257Y mutant presented above are distinct from those described for the salt-bridge mutants. For example, in both mutants the large change in local environment sensed by 140R1 in the dark state is absent. Moreover, the changes in the E134Q mutant did not involve the critical rigid body movement of TM6 required for activation of the protein. In the M257Y mutant, large changes in the local environment were registered by sensors 227R1 and 316R1, but compared with the salt-bridge mutants, the change sensed by 250R1 was small. Site 257 lies two turns of the helix away from the sensor at site 250 on TM6, and a simple interpretation of the above results is that the substitution of Tyr for Met at site 257 causes a steric packing problem at the contact between TM6 and TM2, TM3, and TM7 (see Fig. 1*B*), resulting in a rearrangement that "pushes" TM6 toward the sensor at 227 without completely relieving the tertiary interaction felt by 250.

Mutations That Constitutively Activate Rhodopsin with Bound 11-*cis*-Retinal Inverse Agonist. The double mutants E113Q/M257Y and G90D/M257Y are unique in that they constitutively activate the receptor in the presence of the inverse agonist 11-*cis*-retinal (Table 1). Apparently, the release of the constraint imposed by the salt bridge, either directly or by a competitive mechanism, together with the additional perturbation due to M257Y, is sufficient to achieve an active conformation at the cytoplasmic surface of rhodopsin. This effect is directly mirrored in exaggerated structural changes in E113Q/M257Y and in the absence of additional changes upon light activation.

It is interesting that in the E113Q/M257Y mutant, the EPR spectrum of 227R1 has a signal-to-noise ratio comparable with that of the WT* protein, unlike the low signal-to-noise ratio for comparable quantities of the single salt-bridge mutants. If the low signal-to-noise ratio in E113Q, A292E, and G90D is due to limited accessibility of 227C resulting from the displacement of TM6, as speculated above, one would expect a similar result for E113Q/M257Y, because TM6 movement occurs to an even larger extent. One possible explanation is that in the fully activated structure of the double mutant receptor, large-amplitude, low-frequency fluctuations occur in the structure that permit transient accessibility of 227C for reaction with reagent. Such fluctuations have been previously invoked to explain the apparent accessibility of completely buried cysteines to react with sulfhydryl reagents (27).

Summary. The results presented above directly demonstrate that the K296/E113 salt bridge is an electrostatic switch that when broken through mutagenesis results in a movement of TM6 similar but not identical to that caused by photoactivation in the WT* receptor. Mutations that rupture the salt bridge

trigger an exaggerated motion of TM3, suggesting that a weak interaction may persist between K296 and E113 in the MII state of the WT* receptor, and this interaction is lost in the mutants.

By itself, salt-bridge rupture is insufficient to activate the receptor, and small additional structural changes triggered by isomerization of the 11-*cis* chromophore are required for full activation, indicating that multiple constraints must be modulated to achieve full activation. The double mutant, E113Q/M257Y, achieves nearly full structural and functional activation in the presence of 11-*cis*-retinal. Apparently, the conformation of the protein at the cytoplasmic surface can be uncoupled from chromophore isomerization.

This work was supported by the National Eye Institute, the National Institute of General Medicine, the Jules Stein Professorship Endowment, the Bruce Ford Bundy and Anne Smith Bundy Foundation, and Research to Prevent Blindness.

1. Unger, V. M. & Schertler, G. F. (1995) *Biophys. J.* **68,** 1776–1786.
2. Palczewski, K., Kumasaka, T., Hori, T., Behnke, C. A., Motoshima, H., Fox, B. A., Le Trong, I., Teller, D. C., Okada, T., Stenkamp, R. E., *et al.* (2000) *Science* **289,** 739–745.
3. Teller, D. C., Okada, T., Behnke, C. A., Palczewski, K. & Stenkamp, R. E. (2001) *Biochemistry* **40,** 7761–7772.
4. Okada, T., Fujiyoshi, Y., Silow, M., Navarro, J., Landau, E. M. & Shichida, Y. (2002) *Proc. Natl. Acad. Sci. USA* **99,** 5982–5987.
5. Sakmar, T. P., Franke, R. R. & Khorana, H. G. (1989) *Proc. Natl. Acad. Sci. USA* **86,** 8309–8313.
6. Zhukovsky, E. A. & Oprian, D. D. (1989) *Science* **246,** 928–930.
7. Nathans, J. (1990) *Biochemistry* **29,** 937–942.
8. Emeis, D., Kuhn, H., Reichert, J. & Hofmann, K. P. (1982) *FEBS Lett.* **143,** 29–34.
9. Matthews, R. G., Hubbard, R., Brown, P. K. & Wald, G. (1963) *J. Gen. Physiol.* **47,** 215–240.
10. Rao, V. R. & Oprian, D. D. (1996) *Annu. Rev. Biophys. Biomol. Struct.* **25,** 287–314.
11. Robinson, P. R., Cohen, G. B., Zhukovsky, E. A. & Oprian, D. D. (1992) *Neuron* **9,** 719–725.
12. Cohen, G. B., Oprian, D. D. & Robinson, P. R. (1992) *Biochemistry* **31,** 12592–12601.
13. Dryja, T. P., Berson, E. L., Rao, V. R. & Oprian, D. D. (1993) *Nat. Genet.* **4,** 280–283.
14. Rao, V. R., Cohen, G. B. & Oprian, D. D. (1994) *Nature* **367,** 639–642.
15. Keen, T. J., Inglehearn, C. F., Lester, D. H., Bashir, R., Jay, M., Bird, A. C., Jay, B. & Bhattacharya, S. S. (1991) *Genomics* **11,** 199–205.
16. Govardhn, C. P. & Oprian, D. D. (1994) *J. Biol. Chem.* **269,** 6524–6527.
17. Jin, S., Cornwall, M. C. & Oprian, D. D. (2003) *Nat. Neurosci.* **6,** 731–735.
18. Han, M., Smith, S. O. & Sakmar, T. P. (1998) *Biochemistry* **37,** 8253–8260.
19. Acharya, S. & Karnik, S. S. (1996) *J. Biol. Chem.* **271,** 25406–25411.
20. Cohen, G. B., Yang, T., Robinson, P. R. & Oprian, D. D. (1993) *Biochemistry* **32,** 6111–6115.
21. Hubbell, W. L. & Altenbach, C. (1994) *Curr. Opin. Struct. Biol.* **4,** 566–573.
22. Hubbell, W. L., Mchaourab, H. S., Altenbach, C. & Liezow, M. A. (1996) *Structure (London)* **4,** 779–783.
23. Hubbell, W. L., Gross, A., Langen, R. & Lietzow, M. A. (1998) *Curr. Opin. Struct. Biol.* **8,** 649–656.
24. Feix, J. B. & Klug, C. S. (1998) *Biol. Magn. Reson.* **14**, 251–281.
25. Hubbell, W. L., Cafiso, D. S. & Altenbach, C. (2000) *Nat. Struct. Biol.* **7,** 735–739.
26. Kim, J.-M., Altenbach, C., Thurmond, R. L., Khorana, H. G. & Hubbell, W. L. (1997) *Proc. Natl. Acad. Sci. USA* **94,** 14273–14278.
27. Hubbell, W. L., Altenbach, C., Hubbell, C. M. & Khorana, H. G. (2003) *Adv. Protein Chem.* **63,** 243–290.
28. Altenbach, C., Yang, K., Farrens, D. L., Farahbakhsh, Z. T., Khorana, H. G. & Hubbell, W. L. (1996) *Biochemistry* **35,** 12470–12478.
29. Farrens, D. L., Altenbach, C., Yang, K., Hubbell, W. L. & Khorana, H. G. (1996) *Science* **2274,** 768–777.
30. Sheikh, S. P., Zvyaga, T. A., Lichtarge, O., Sakmar, T. P. & Bourne, H. R. (1996) *Nature* **383,** 347–350.
31. Farahbakhsh, Z. T., Ridge, K., Khorana, H. G. & Hubbell, W. L. (1995) *Biochemistry* **34,** 8812–8819.
32. Resek, J. F., Farahbakhsh, Z. T., Hubbell, W. L. & Khorana, H. G. (1993) *Biochemistry* **32,** 12025–12032.
33. Yang, K., Farrens, D. L., Hubbell, W. L. & Khorana, H. G. (1996) *Biochemistry* **35,** 12464–12469.
34. Oprian, D. D., Molday, R. S., Kaufman, R. J. & Khorana, H. G. (1987) *Proc. Natl. Acad. Sci. USA* **84,** 8874–8878.
35. Baehr, W., Morita, E. A., Swanson, R. J. & Applebury, M. L. (1982) *Hoppe-Seyler's Z. Physiol. Chem.* **257,** 6452–6460.
36. Fahmy, K. & Sakmar, T. P. (1993) *Biochemistry* **32,** 7229–7236.
37. Cai, K., Klei-Seetharaman, J., Altenbach, C., Hubbell, W. L. & Khorana, H. G. (2001) *Biochemistry* **40,** 12479–12485.
38. Zvyaga, T. A., Fahmy, K., Siebert, F. & Sakmar, T. P. (1996) *Biochemistry* **35,** 7536–7545.